The transcriptional repressor CDP (Cutl1) is essential for epithelial cell differentiation of the lung and the hair follicle

Tammy Ellis,[1,4] Laure Gambardella,[2,4] Markus Horcher,[1] Stefan Tschanz,[3] Janine Capol,[3] Paula Bertram,[1] Wolfram Jochum,[1,5] Yann Barrandon,[2] and Meinrad Busslinger[1,6]

[1]Research Institute of Molecular Pathology, Vienna Biocenter, A-1030 Vienna, Austria; [2]Department of Biology, École Normale Supérieure, F-75230 Paris, France; [3]Institute of Anatomy, University of Bern, CH-3000 Bern, Switzerland

The mammalian *Cutl1* gene codes for the CCAAT displacement protein (CDP), which has been implicated as a transcriptional repressor in diverse processes such as terminal differentiation, cell cycle progression, and the control of nuclear matrix attachment regions. To investigate the in vivo function of *Cutl1*, we have replaced the C-terminal Cut repeat 3 and homeodomain exons with an in-frame *lacZ* gene by targeted mutagenesis in the mouse. The CDP–lacZ fusion protein is retained in the cytoplasm and fails to repress gene transcription, indicating that the *Cutl1^{lacZ}* allele corresponds to a null mutation. *Cutl1* mutant mice on inbred genetic backgrounds are born at Mendelian frequency, but die shortly after birth because of retarded differentiation of the lung epithelia, which indicates an essential role of CDP in lung maturation. A less pronounced delay in lung development allows *Cutl1* mutant mice on an outbred background to survive beyond birth. These mice are growth-retarded and develop an abnormal pelage because of disrupted hair follicle morphogenesis. The inner root sheath (IRS) is reduced, and the transcription of *Sonic hedgehog* and IRS-specific genes is deregulated in *Cutl1* mutant hair follicles, consistent with the specific expression of *Cutl1* in the progenitors and cell lineages of the IRS. These data implicate CDP in cell-lineage specification during hair follicle morphogenesis, which resembles the role of the related Cut protein in specifying cell fates during *Drosophila* development.

[*Key Words*: CCAAT displacement protein; Cux; Cutl1; lung; hair follicle development]

Received February 6, 2001; revised version accepted July 13, 2001.

The CCAAT displacement protein (CDP) was discovered as a sea urchin transcription factor that restricts expression of the sperm *H2B* gene to spermatocytes by binding to the CCAAT promoter element in somatic tissues and thereby preventing access of transcriptional activators to the *H2B* promoter (Barberis et al. 1987). The human CDP (Superti-Furga et al. 1988) was next shown to act as a repressor of the myelomonocytic *gp91^{phox}* gene (Skalnik et al. 1991) and, upon biochemical purification, was identified as a homolog of the *Drosophila* homeodomain protein Cut (Neufeld et al. 1992). CDP, which is also known as Cux1 (Cut homeobox-1), and its related Cux2 protein were subsequently isolated from several different vertebrate species (for review, see Nepveu 2001). The *Drosophila* Cut protein and its vertebrate homologs share a conserved coiled-coil region at the N terminus, three internal 60-amino-acid repeats (known as Cut repeats), and a divergent homeodomain located near the C terminus (Fig. 1B; Blochlinger et al. 1988; Neufeld et al. 1992). The mammalian *CDP/Cux1* locus is large and complex, giving rise to at least six different splice products as a result of alternative transcription initiation, splicing, and polyadenylation (Vanden Heuvel et al. 1996; Lievens et al. 1997; Zeng et al. 2000). One of these splice products corresponds to the nuclear protein CASP (CDP alternative splice product), which shares with CDP only the N-terminal coiled-coil sequences (Fig. 1B; Lievens et al. 1997). Here we refer to the mammalian locus as *Cutl1* (*Cut-like 1*) and to its two most prominent protein isoforms as CDP and CASP.

The CDP protein contains four different DNA-binding domains because each of the three Cut repeats is capable of DNA sequence recognition in addition to the homeodomain (for review, see Moon et al. 2000). The presence of multiple DNA-binding modules results in a

[4]These authors contributed equally to this work.
[5]Present address: Institute of Clinical Pathology, University Hospital, Schmelzbergstrasse 12, CH-8091 Zürich, Switzerland.
[6]Corresponding author.
E-MAIL Busslinger@nt.imp.univie.ac.at; FAX 43/1-798-93-70.
Article and publication are at http://www.genesdev.org/cgi/doi/10.1101/gad.200101.

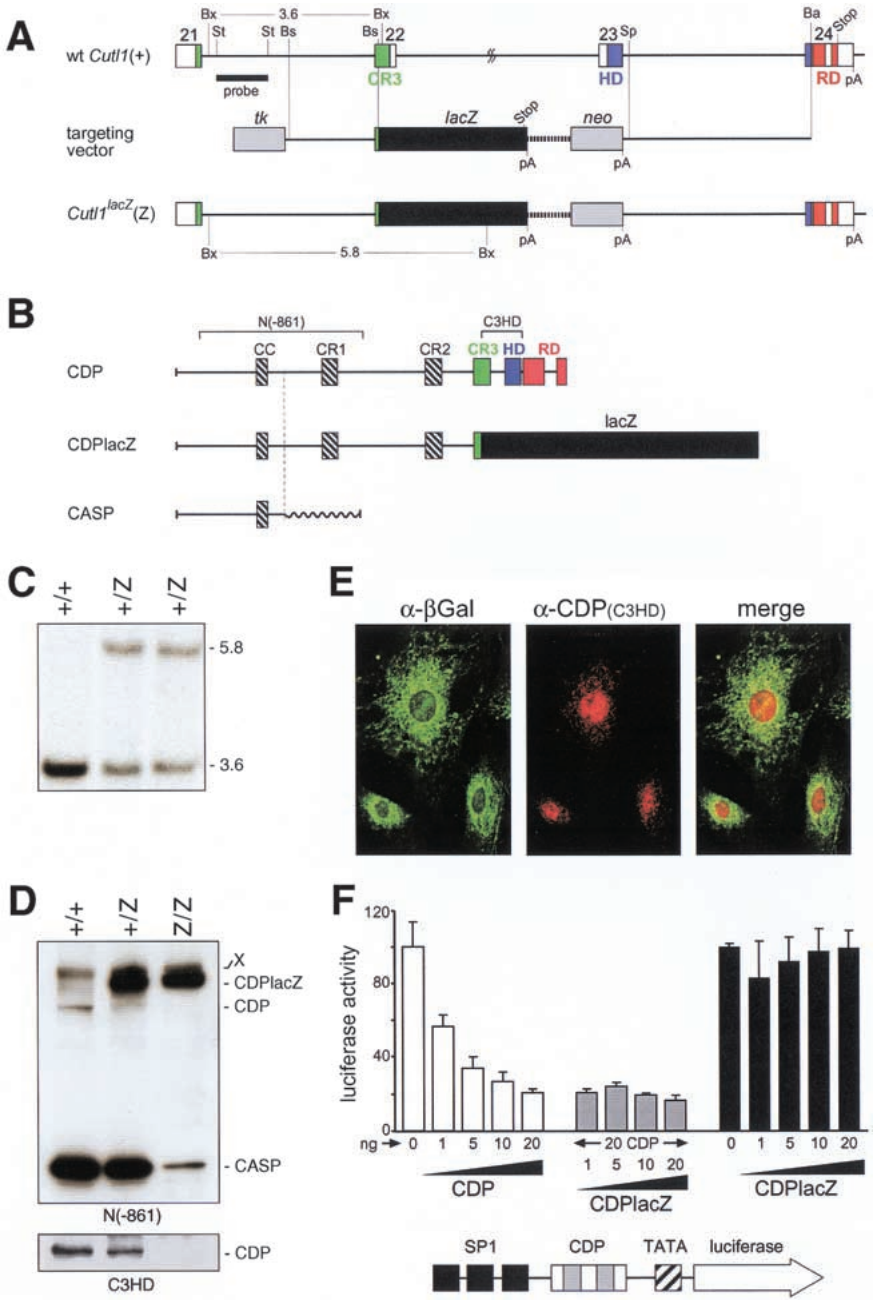

Figure 1. Generation of the *Cutl1*^{Z} allele. (*A*) Structure of the wild-type and targeted *Cutl1* loci. The targeting vector is shown together with the genomic structure of exons 21–24 (numbered according to Zeng et al. 2000). Correct targeting was verified by Southern blot analysis of *Bst*XI-digested DNA with the indicated probe. The lengths of the *Bst*XI fragments are shown in kilobases. (Ba) *Bam*HI; (Bs) *Bsa*I; (Bx) *Bst*XI; (Sp) *Sph*I; (St) *Sty*I; (pA) polyadenylation site; (CR3) Cut repeat 3; (HD) homeodomain; (RD) repression domain; (neo) neomycin; (tk) thymidine kinase. (*B*) Schematic diagram of the different proteins encoded by the *Cutl1* loci. The epitopes recognized by the N[-861] and C3HD antibodies are indicated. (CC) Coiled-coil region. (*C*) Southern blot analysis of *Bst*XI-digested DNA from *Cutl1*$^{+/Z}$ offspring. (*D*) Western blot analysis. Low-salt protein extracts of primary embryo fibroblasts were analyzed by immunoblotting with the N[-861] and C3HD antibodies. The nuclear CDP protein was only partially extracted at 120 mM KCl in contrast to the cytoplasmic CDP–lacZ protein. (X) Cross-reacting protein. (*E*) Subcellular localization of CDP proteins. *Cutl1*$^{+/Z}$ fibroblasts were simultaneously stained with anti-CDP (C3HD) and anti-β-galactosidase antibodies. (*F*) Absence of transcriptional repression by CDP–lacZ. The CDP and/or CDP–lacZ expression plasmids (1–20 ng) were transiently transfected into NIH 3T3 cells together with the SP1-γ–TATA–luciferase gene (100 ng, shown below) and the *Renilla* luciferase construct pRL–SV40 (10 ng). After 48 h, the activity of the firefly luciferase was measured and standardized relative to that of the control *Renilla* luciferase. Average values of six experiments are shown relative to the activity measured with the empty expression vector pRK5 (100%, *left* bar). The CDP and CDP–lacZ proteins were expressed at similar levels (data not shown).

highly flexible mode of sequence recognition, thus providing an explanation for the ability of CDP to bind to a large spectrum of different DNA sequences (Moon et al. 2000). Once bound to DNA, CDP represses target gene transcription by two distinct mechanisms. In one mechanism, it interferes with the binding of transcriptional activators by competing for binding-site occupancy (Barberis et al. 1987; Skalnik et al. 1991; Mailly et al. 1996). This CCAAT-displacement activity is mediated by the Cut repeats 1 and 2 (Moon et al. 2000). Alternatively, the CDP protein can actively repress gene transcription through its C-terminal sequences, which bind to and thus recruit histone deacetylases (HDAC) to target gene promoters (Mailly et al. 1996; Li et al. 1999).

Protein–DNA binding studies and functional promoter analyses have implicated the CDP protein in the regulation of a large variety of cellular and viral genes, including the *gp91*^{phox}, c-*myc*, c-*mos*, *N-cam*, *CFTR*, *p21*$^{WAF1/CIP1}$, *lactoferrin*, *tyrosine hydroxylase*, *thymidine kinase*, and *histone* genes (for review, see Nepveu 2001). Although these genes have not been genetically verified to be endogenous targets of CDP, their functions have led to several hypotheses concerning the in vivo role of CDP. The inverse correlation between the expression of the CDP repressor and its target gene *gp91*^{phox} during myeloid differentiation has led to the hypothesis that CDP functions in lineage-committed precursor cells to repress genes, which are activated only during the CDP-negative

phase of terminal differentiation (Skalnik et al. 1991; Lievens et al. 1995; Wang et al. 1999). An alternative, but not mutually exclusive function implicates CDP in the control of cell-cycle progression based on the following evidence. First, the DNA-binding activity of CDP was shown to oscillate during the cell cycle, reaching maximal levels during late G_1 and the S phase (Coqueret et al. 1998). Second, CDP was identified as the DNA-binding component of the cell-cycle-regulated, Rb-containing transcription factor complex HiNF-D (van Wijnen et al. 1996). Third, several of the putative CDP target genes (see above) are regulated in a cell-cycle-dependent manner. Finally, CDP has also been proposed to function as an architectural protein, as it binds to and negatively regulates nuclear matrix attachment regions in the *CD8*α, T cell receptor β (*TCR*β), and immunoglobulin heavy-chain (*IgH*) loci (Banan et al. 1997; Chattopadhyay et al. 1998; Wang et al. 1999).

Genetic studies revealed different functions of the *cut* gene during *Drosophila* development. Loss- and gain-of-function analysis showed that Cut is not only necessary but also sufficient for specifying the identity of external sensory organs during peripheral nervous system development (Blochlinger et al. 1988, 1991). However, Cut also fulfills non-cell-autonomous functions during the formation of the egg chamber and wing margin, where it is involved in the control of intercellular communication (Jackson and Blochlinger 1997; Micchelli et al. 1997). Interestingly, ectopic expression of the mammalian CDP protein in *Drosophila* was able to rescue the *cut wing* mutant phenotype, indicating that the function of Cut and CDP proteins has been conserved in evolution (Ludlow et al. 1996).

Here we have analyzed the in vivo function of the mouse *Cutl1* gene by targeted replacement of the Cut repeat 3 and homeodomain exons with an in-frame *lacZ* gene, which resulted in a transcriptionally inactive fusion protein. Homozygous mutant mice on inbred genetic backgrounds died at birth from respiratory failure, which was caused by retarded differentiation of the lung epithelia. This delay in lung development was less pronounced in *Cutl1* mutant mice on an outbred background, which survived but were growth-retarded. These mice had a sparse pelage of abnormal hair caused by severe impairment of hair follicle development. The cell layers of the inner root sheath (IRS) were reduced in *Cutl1* mutant hair follicles, consistent with the finding that *Cutl1* is selectively expressed in the progenitors and cell lineages of the IRS. Moreover, the expression of *Sonic hedgehog* and IRS-specific genes was deregulated in *Cutl1* mutant hair follicles. These data indicate a role of CDP in cell lineage specification of the hair follicle in analogy with the selector function of *Drosophila* Cut in the peripheral nervous system.

Results

Targeted mutation of the Cutl1 *gene*

The mammalian *Cutl1* locus is highly complex, as it spans at least 340 kb of genomic DNA, codes for 33 exons, is transcribed from different promoters, and gives rise to several alternative splice products (Vanden Heuvel et al. 1996; Lievens et al. 1997; Tufarelli et al. 1998; Zeng et al. 2000). However, all CDP isoforms end with the same C-terminal sequences containing the DNA-binding regions of the Cut repeat 3 and homeodomain as well as two repression domains. Because these functional domains are essential for the DNA-binding and repression activities of CDP (Nepveu 2001), we chose to inactivate the *Cutl1* gene by targeting these C-terminal sequences (Fig. 1A). Moreover, as the developmental expression pattern of the *Cutl1* gene is only partially known, we inserted a *lacZ* (*Z*) gene in-frame into *Cutl1* exon 22 to be able to follow the expression of the targeted allele by β-galactosidase staining (Fig. 1A). Correctly targeted ES cells were injected into blastocysts to generate heterozygous $Cutl1^{+/Z}$ mice (Fig. 1C), which were indistinguishable from their wild-type littermates with regard to viability, growth, behavior, and fertility.

To characterize the $Cutl1^{Z}$ mutation molecularly, we cultured primary fibroblasts from wild-type and *Cutl1* mutant embryos and subsequently analyzed protein extracts of these cells by Western blotting (Fig. 1D). An antibody recognizing N-terminal CDP sequences (N[-861]) detected both the full-length CDP protein (180 kD) and the alternative splice product CASP (80 kD) in wild-type fibroblasts. In contrast, homozygous $Cutl1^{Z/Z}$ fibroblasts expressed the larger CDP–lacZ fusion protein (250 kD) instead of full-length CDP. Expression of the CASP protein was maintained in these fibroblasts, although at a sixfold lower level (Fig. 1D), which could reflect a decrease in alternative splicing of the *CASP* transcript. The presence of two additional polyadenylation sites between exons 22 and 24 of the targeted *Cutl1* allele (Fig. 1A) may, indeed, increase the efficiency of polyadenylation in this region and thus interfere with alternative splicing of the primary transcript from exon 14 to the downstream exons 25–33 coding for the unique C-terminal sequences of CASP (Fig. 1B; Lievens et al. 1997; Zeng et al. 2000).

We investigated the subcellular localization of the CDP and CDP–lacZ proteins by immunostaining of heterozygous $Cutl1^{+/Z}$ fibroblasts. An antibody (C3HD) that recognizes the Cut repeat 3 and homeodomain sequences deleted in the $Cutl1^{Z}$ allele (Fig. 1B) localized the wild-type CDP protein predominantly in the nucleus of $Cutl1^{+/Z}$ fibroblasts (Fig. 1E). Surprisingly, however, the CDP–lacZ protein was excluded from the nucleus, as it was detected with an anti-βGal antibody in the cytoplasm of the same fibroblasts. Hence, the CDP–lacZ protein is sequestered away from the nucleus, where CDP normally functions to regulate gene transcription.

The transcriptional activity of the wild-type CDP and CDP–lacZ fusion proteins was next compared in transiently transfected NIH 3T3 cells. As shown in Figure 1F, increasing amounts of exogenous CDP protein efficiently repressed the activity of a cotransfected SP1-γ–TATA–luciferase gene (Lievens et al. 1995), in marked contrast to the CDP–lacZ protein. Moreover, coexpression of CDP–lacZ failed to interfere with the repression

function of CDP, thus excluding a dominant-negative function of the fusion protein. In summary, the lack of repression activity and the cytoplasmic location of the CDP–lacZ protein strongly argue that the targeted mutation abrogates the transcriptional function of CDP and therefore corresponds to a null allele.

Postnatal lethality and growth retardation of Cutl1 *mutant mice*

Intercrosses of heterozygous mutant mice showed that *Cutl1*$^{Z/Z}$ mice are born at the expected Mendelian frequency, indicating that the *Cutl1*^{Z} mutation does not interfere with embryonic development. However, the *Cutl1*$^{Z/Z}$ mice died shortly after birth from respiratory failure. This early postnatal lethality was observed with *Cutl1*$^{Z/Z}$ mice that were bred on the C3H/He or C57BL/6 × 129/Sv strain background. A few *Cutl1*$^{Z/Z}$ mice (~1%) on the latter genetic background survived beyond birth, but then were severely growth-retarded and had only a sparse pelage of abnormal hair (Fig. 2A,B). In marked contrast, the majority of *Cutl1*$^{Z/Z}$ mice survived on the outbred OF1 background, but were still growth-retarded (Fig. 2C). Because abnormal function of the pituitary or thyroid glands could explain the observed growth retardation, we measured the levels of growth hormone (GH) and thyroid-stimulating hormone (TSH) in the blood of 2-week-old *Cutl1*$^{Z/Z}$ mice. Growth hormone was present in the sera of mutant (n = 8) and wild-type (n = 6) mice at 5.3 and 7.0 ng/mL and TSH at 138 and 118 ng/mL, respectively. Therefore, the normal synthesis of these hormones indicates that the observed growth retardation of *Cutl1*$^{Z/Z}$ mice is not caused by dysfunction of the thyroid or pituitary glands, although *Cutl1* is expressed during the development of these organs (see below).

Cutl1 *expression during development*

We next analyzed the developmental expression pattern of *Cutl1* by β-galactosidase staining of mutant embryos. *Cutl1* expression was detected in most tissues at embryonic day 8.5 (E8.5) and, starting with E12.5, became gradually restricted to a subset of organs (data not shown). The *Cutl1* gene was specifically expressed in the epithelial compartment of the developing whisker, tooth, choroid plexus, Rathke's pouch (pituitary), thyroid, salivary gland, pancreas, kidney, and lung (Figs. 2D–H, 3A,B; data not shown). In addition, *Cutl1* was also expressed in striated and smooth muscles of various organs (Fig. 2G,I) and in hypertrophic chondrocytes of developing bones (data not shown).

The *Cutl1* gene is most highly expressed in the testis among all tissues of adult males (Vanden Heuvel et al. 1996). Consistent with this finding, β-galactosidase staining was detected in the postmeiotic round and elongating spermatids, but neither in spermatocytes, elongated spermatids, nor mature sperm in the testes of heterozygous males (Fig. 2J). Surprisingly, however, matings of *Cutl1*$^{Z/Z}$ OF1 males with wild-type females resulted

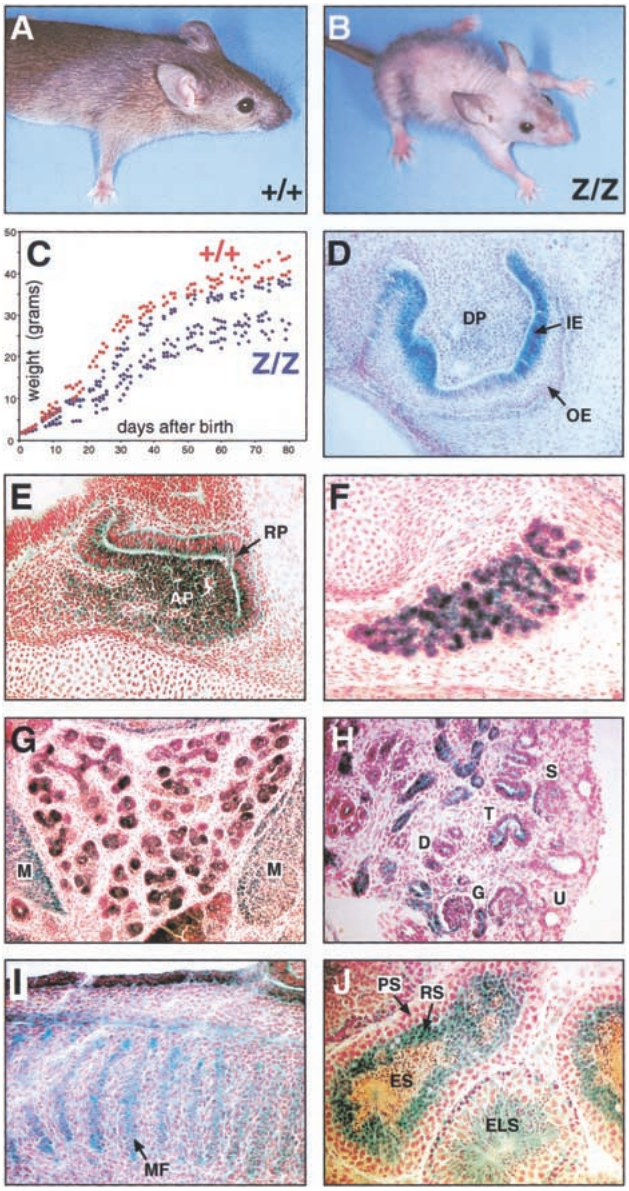

Figure 2. Growth retardation and expression analysis of *Cutl1* mutant mice. (*A*,*B*) View of a wild-type mouse (*A*) and its surviving *Cutl1*$^{Z/Z}$ littermate (*B*) (on the C57BL/6 × 129/Sv background) at postnatal day 37. (*C*) Delayed growth of *Cutl1*$^{Z/Z}$ mice maintained on the OF1 background. The weight of wild-type (n = 3) and *Cutl1*$^{Z/Z}$ (n = 6) mice was measured at regular intervals after birth. (*D–J*) *Cutl1* expression in the developing incisor tooth (*D*), pituitary (*E*), thyroid (*F*), salivary gland (*G*), kidney (*H*), tongue muscle (*I*), and testis (*J*). X-Gal staining was performed on cryosections of *Cutl1*$^{Z/Z}$ fetuses at day 14.5 (*D*,*E*, *I*) or day 16.5 (*F–H*) and of the testis of a 3-month-old *Cutl1*$^{+/Z}$ mouse (*J*). (AP) Anterior pituitary; (D) collecting duct; (DP) dental papilla; (ELS) elongating spermatid; (ES) elongated spermatid; (G) glomerulus; (IE) inner enamel epithelium; (M) muscle; (MF) muscle fiber; (OE) outer enamel epithelium; (PS) pachytene spermatocyte; (RP) Rathke's pouch; (RS) round spermatid; (S) S-shaped body; (T) tubule; (U) ureteric tip.

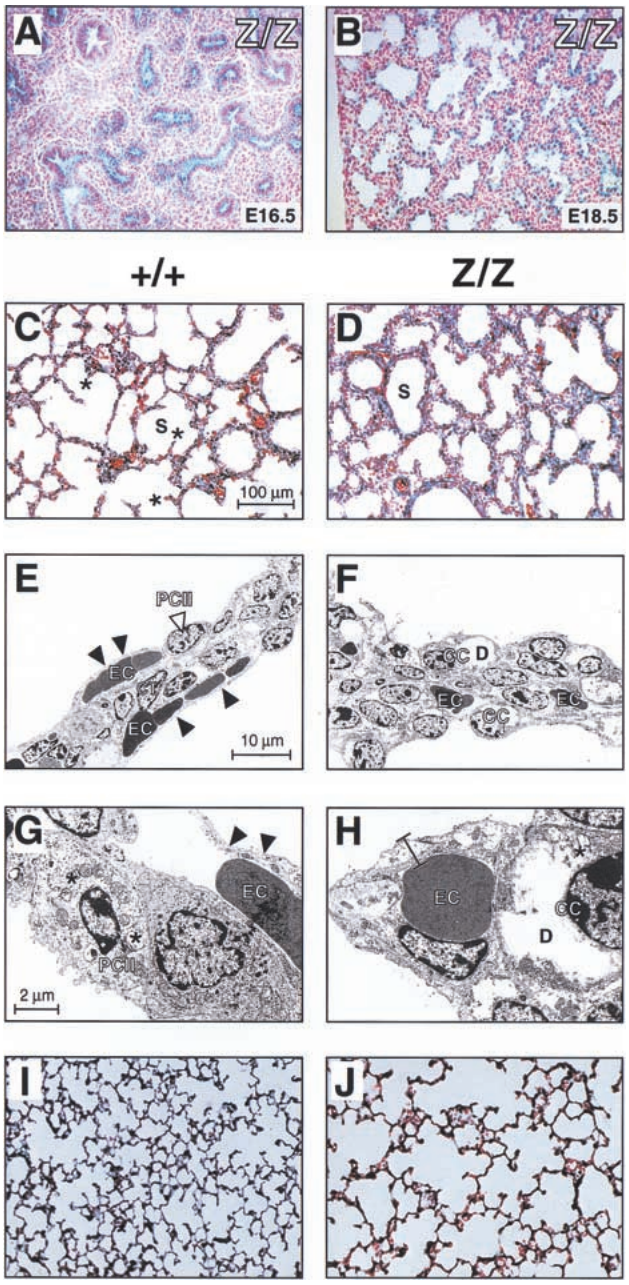

Figure 3. Developmental abnormalities of the *Cutl1* mutant lung. (*A*,*B*) β-Galactosidase staining of lung cryosections from *Cutl1*$^{Z/Z}$ fetuses at days 16.5 and 18.5. (*C*,*D*,*I*,*J*) Histological analysis of inflated lungs at birth (*C*,*D*) and postnatal day 21 (*I*,*J*). Asterisks denote the outgrowth of secondary septa within the saccules (S). (*E–H*) Transmission electron micrographs of lung septa at birth. The septa of the *Cutl1*$^{Z/Z}$ mouse (*F*,*H*) are composed of cuboidal epithelial cells (CC), which contain large deposits (D) of loose material (probably glycogen), as shown at high magnification (*H*). In contrast, the wild-type lung (*E*,*G*) consists of type I and II pneumocytes (PC) and two layers of erythrocyte (EC)-containing capillaries that are separated by connective tissue (CT). The type II pneumocytes contain many lamellar bodies (asterisks). Arrowheads point to the thin blood–air barrier, which is composed of type I pneumocytes and endothelial cells of the capillary. All analyses were performed with mice on the C57BL/6 × 129/Sv background.

in litters of normal size, demonstrating that the *Cutl1*^{Z} mutation does not impair male fertility.

Retardation of lung development in Cutl1 *mutant mice*

Histological examination of newborn *Cutl1*$^{Z/Z}$ mice revealed morphological abnormalities in the lung and skin. During lung development, *Cutl1* expression was first observed in the columnar epithelium of the bronchioles at E12.5, was increased during the canalicular and saccular stages of lung morphogenesis (E16.5–E18.5), and then became undetectable in the mature lung at 3 wk of age (Fig. 3A,B; data not shown). Consistent with this expression pattern, *Cutl1*$^{Z/Z}$ mice on inbred backgrounds became cyanotic shortly after birth despite normal respiratory muscle contractions and died within 2–6 h from lung failure. This *Cutl1* mutant phenotype resembles the respiratory distress syndrome of human infants, wherein inadequate surfactant levels do not allow proper inflation of the immature lung (Burri 1999). In contrast to the human condition, however, *Cutl1*$^{Z/Z}$ pups could not be rescued by intraperitoneal injection of dexamethasone into pregnant females at days 16.5–18.5 of gestation. Moreover, quantitative RT–PCR analyses revealed that the surfactant genes *SP-A*, *SP-B*, and *SP-C* were normally transcribed in *Cutl1*$^{Z/Z}$ lungs at birth (data not shown).

Histological and electron microscopic analyses revealed a lower complexity of the lung parenchyma in newborn *Cutl1*$^{Z/Z}$ mice compared with wild-type littermates (Fig. 3C,D). At birth, wild-type lungs are at the late saccular stage, which is characterized by septa containing two layers of capillaries on either side of a thin axial sheath of interstitial cells (Fig. 3C,E). Flat type I pneumocytes and capillary endothelial cells (Fig. 3E,G, arrowheads) constitute a thin blood–air barrier facilitating an efficient gas exchange, and the septa contain type II pneumocytes with their characteristic lamellar bodies, which are involved in the storage and exocytosis of surfactant proteins (Fig. 3G). The growth of secondary septa (Fig. 3C, asterisks) has started to subdivide the lumen of the saccules, thus initiating the process of alveolization. In marked contrast, the septa of newborn *Cutl1*$^{Z/Z}$ lungs were still thick, with a broad interstitial cell layer and a loose arrangement of capillaries (Fig. 3D,F). The septal walls were very smooth and formed round saccules lacking any outgrowth of secondary septa (Fig. 3D). Instead of type I and II pneumocytes, the *Cutl1*$^{Z/Z}$ septa contained many cuboidal cells, which are considered to be pneumocyte precursors (Fig. 3F,H). In summary, the lungs of *Cutl1*$^{Z/Z}$ newborns displayed morphological features normally seen only at the beginning of the saccular stage, indicating that the lack of *Cutl1* function leads to a maturation delay of 2 d. The observed retardation results in the absence of a mature blood–air barrier at birth and is most likely responsible for the respiratory failure of newborn *Cutl1*$^{Z/Z}$ pups on inbred strain backgrounds.

Analysis of adult *Cutl1*$^{Z/Z}$ survivors revealed that the lungs of these mice contained fully differentiated type I and type II pneumocytes, a well-developed blood–air barrier, and a mature microvasculature. However, the air

spaces were markedly dilated, and the lungs displayed a decreased complexity of the alveolar network as a consequence of delayed initiation and/or incomplete execution of the alveolar differentiation program (Fig. 3J). Therefore, we conclude that *Cutl1* is essential for proper maturation of the lung.

Defective hair formation in Cutl1 *mutant mice*

The absence of a normal hair coat was a consistent and background-independent phenotype of all surviving $Cutl1^{Z/Z}$ mice (Fig. 2B). A defect in hair follicle development was already apparent at birth, as $Cutl1^{Z/Z}$ pups were born with only a few stunted and curly whiskers (Fig. 4B). These mice initially developed a rudimentary hair coat, but after 1 wk started to lose most of their pelage hair (Fig. 2B). This phenotype was also recapitulated in grafts of newborn $Cutl1^{Z/Z}$ skin that were transplanted onto athymic (*nu/nu*) mice. The $Cutl1^{Z/Z}$ skin grafts developed only sparse, short, and disorganized hair (Fig. 4D) in contrast to the dense fur generated by wild-type skin grafts (Fig. 4C). The hair coat of a wild-type mouse is composed of four different hair types known as guard, awl, auchene, and zig-zag hair (Philpott and Paus 1998). These hair types could not be identified in the $Cutl1^{Z/Z}$ skin, which instead gave rise to all major hair abnormalities found in different human skin diseases (Whiting 1994). The same $Cutl1^{Z/Z}$ pelage contained twisted, bifurcated, circle, and corkscrew hair as well as hair with nodules or longitudinal grooving (Fig. 4E–J). Furthermore, electron microscopy showed that scales were absent on the *Cutl1* mutant hair, which may reflect abnormal development of the cuticle cell layers in the hair follicle (Fig. 4L).

The hair follicles initially developed normally and are present in correct numbers in the dorsal skin of 18.5-day-old $Cutl1^{Z/Z}$ fetuses (Fig. 5A,B). In contrast, their morphogenesis was severely disrupted in 3-week-old $Cutl1^{Z/Z}$ mice (Fig. 5C,D). Most hair follicles were extremely misoriented, often appeared cystic or even sclerotic, and contained more than one degenerated hair shaft (Fig. 5D,E). The viable hair follicles expressed the $Cutl1^{lacZ}$ gene in all cell layers except in the outer root sheath and dermal papilla (Fig. 5E,F). Importantly, the hair follicles in the $Cutl1^{Z/Z}$ skin grafts were equally disorganized (data not shown), demonstrating that the disruption of hair development is caused by a skin-autonomous defect.

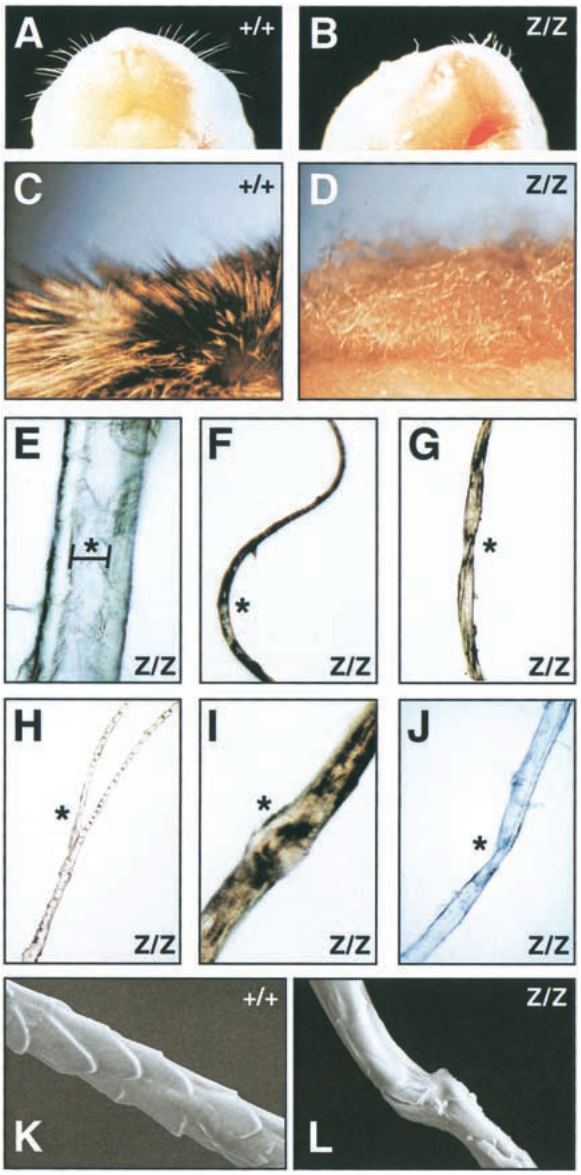

Figure 4. Aberrant hair formation in *Cutl1* mutant mice. (*A*,*B*) View of the snout of newborn wild-type and $Cutl1^{Z/Z}$ mice. (*C*,*D*) Close-up view of the fur of a wild-type (*C*) and $Cutl1^{Z/Z}$ (*D*) skin graft at 6 wk after transplantation onto an athymic (*nu/nu*) mouse. (*E–J*) Multiple abnormalities of pelage hair taken from the same $Cutl1^{Z/Z}$ skin graft. Hair with longitudinal grooving (bracket in *E*), circle hair (*F*), pili torti (*G*), bifurcated hair (*H*), trichorrhexis nodosa (*I*), and corkscrew hair (*J*). Asterisks indicate the different hair abnormalities. (*K*,*L*) Scanning electron micrograph of pelage hair. Scales are absent on the surface of the *Cutl1* mutant hair (*L*) in contrast to wild-type hair (*K*).

Abnormal differentiation of the inner root sheath in Cutl1 *mutant hair follicles*

We next studied the expression of the *Cutl1* gene in the whisker follicle, which, as the largest of all hair follicles, provides the highest cellular resolution. The dermal papilla of the whisker follicle is surrounded by an epithelial core that is composed of several concentric cell layers comprising the outer root sheath (ORS), inner root sheath (IRS), and hair shaft (Fig. 6D). Each layer consists of different cell lineages, which are derived from the same multipotent stem cell located in the bulge of the hair follicle. This stem cell migrates from the bulge through the basal layer of the ORS to the matrix region of the hair bulb, where it becomes committed to one of the distinct cell lineages of the hair follicle (Fig. 6D; Tay-

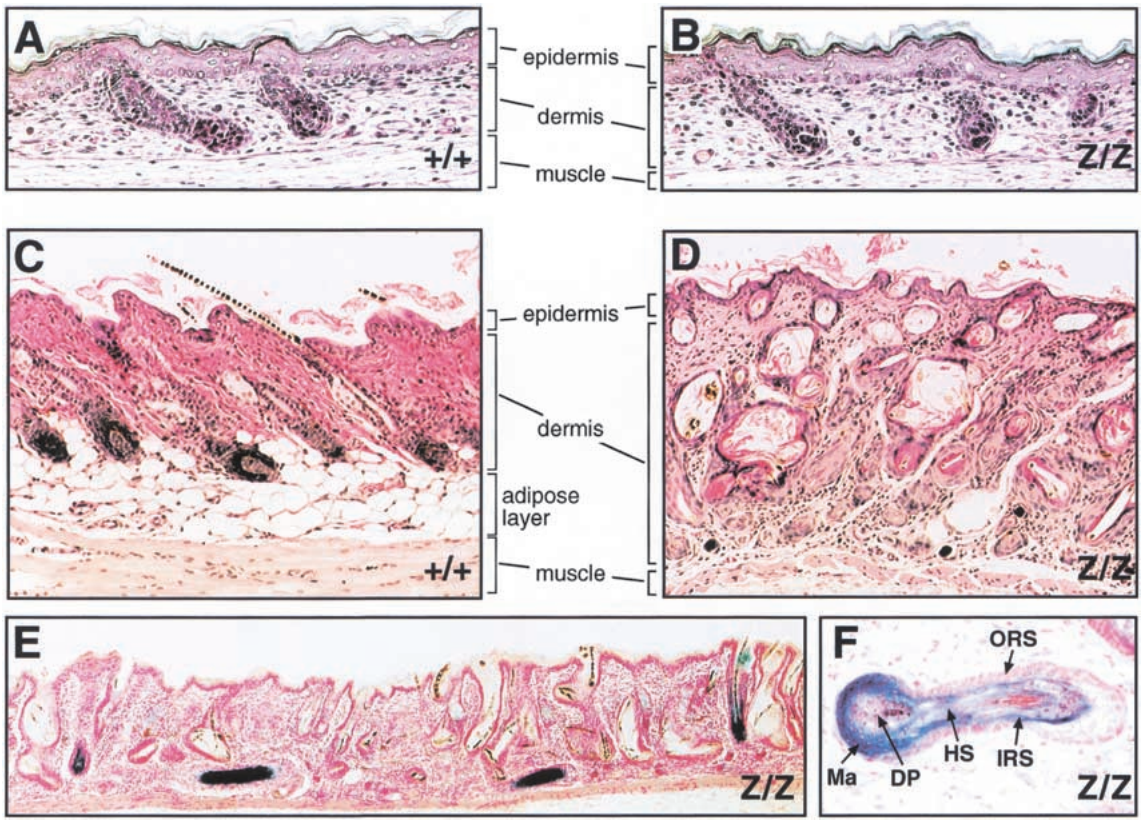

Figure 5. Disruption of hair follicle development in the skin of *Cutl1* mutant mice. (*A–D*) Histological analysis of the skin from wild-type and $Cutl1^{Z/Z}$ mice at E18.5 (*A*,*B*) and postnatal day 21 (*C*,*D*), respectively. (*E*) β-Galactosidase staining of a skin section from a 20-day-old $Cutl1^{Z/Z}$ mouse. (*F*) Higher magnification of an X-gal-stained $Cutl1^{Z/Z}$ hair follicle that grew parallel to the epidermal surface. *Cutl1* mutant survivors on the C57BL/6 × 129/Sv background were analyzed. (DP) Dermal papilla; (HS) hair shaft; (IRS) inner root sheath; (Ma) matrix; (ORS) outer root sheath.

lor et al. 2000; Oshima et al. 2001). Immunohistochemical staining of a wild-type whisker follicle with an anti-CDP antibody showed that *Cutl1* is not expressed in the upper part of the ORS (Fig. 6A,B), but is activated in keratinocytes arriving in the ORS of the bulb (Fig. 6C). *Cutl1* expression is subsequently maintained in the IRS progenitor cells of the matrix, in the three layers of the differentiating IRS (cuticle, Huxley's and Henlé's layers), and in the companion cell layer (Fig. 6A,B). The *Cutl1* gene is, however, down-regulated in progenitors of the hair shaft and is subsequently not expressed in the three cell lineages constituting the hair (Fig. 6A–D). Consistent with this expression pattern, the differentiation of IRS cells was impaired in $Cutl1^{Z/Z}$ whisker follicles (Fig. 6E,F). The cell layers of the IRS were reduced, whereas the ORS was enlarged, possibly as a secondary consequence of the alterations in the IRS. The absence of CDP did not, however, interfere with cell proliferation in the matrix region, as evidenced by the presence of many mitotic cells in the bulb of $Cutl1^{Z/Z}$ follicles (Fig. 6F).

To investigate the molecular basis of the *Cutl1* mutant phenotype, we compared the expression of IRS-specific genes in wild-type and mutant whisker follicles. Interestingly, the $Cutl1^{lacZ}$ gene itself was expressed, in addition to the IRS, also in the cortex of homozygous CDP-deficient follicles in marked contrast to heterozygous CDP-expressing follicles (Fig. 7D). Moreover, the cytokeratin K6hf, which is specifically expressed in the companion cell layer of wild-type follicles (Winter et al. 1998), was detected throughout the IRS as well as in the cortex of $Cutl1^{Z/Z}$ follicles (Fig. 7E). Likewise, the IRS-specific cytokeratin K6irs and keratin-associated trichohyalin protein were misexpressed in the cortex of mutant hair follicles (Fig. 7A; data not shown). Therefore, these results indicate that the loss of CDP leads to deregulated expression of IRS-specific genes in the hair shaft.

However, the $Cutl1^{Z}$ mutation did not affect the regulation of genes that are expressed during differentiation of the hair-shaft lineages. Expression of the hair keratin Hacl-1 and the transcription factor Foxn1 (Whn) also remained restricted to the cortex in mutant hair follicles (Fig. 7B,C). Moreover, we did not observe any difference in gene expression of the hair keratin MHKA-1; the transcription factors Lef1, Msx2, and Hairless; the Notch1 receptor; and the secreted proteins Bmp2, Bmp4, and Wnt3a between wild-type and mutant follicles (data not shown). Importantly, however, the expression of the signaling molecule Sonic hedgehog (Shh) was deregulated in the absence of CDP. Whereas *Shh* is expressed in small

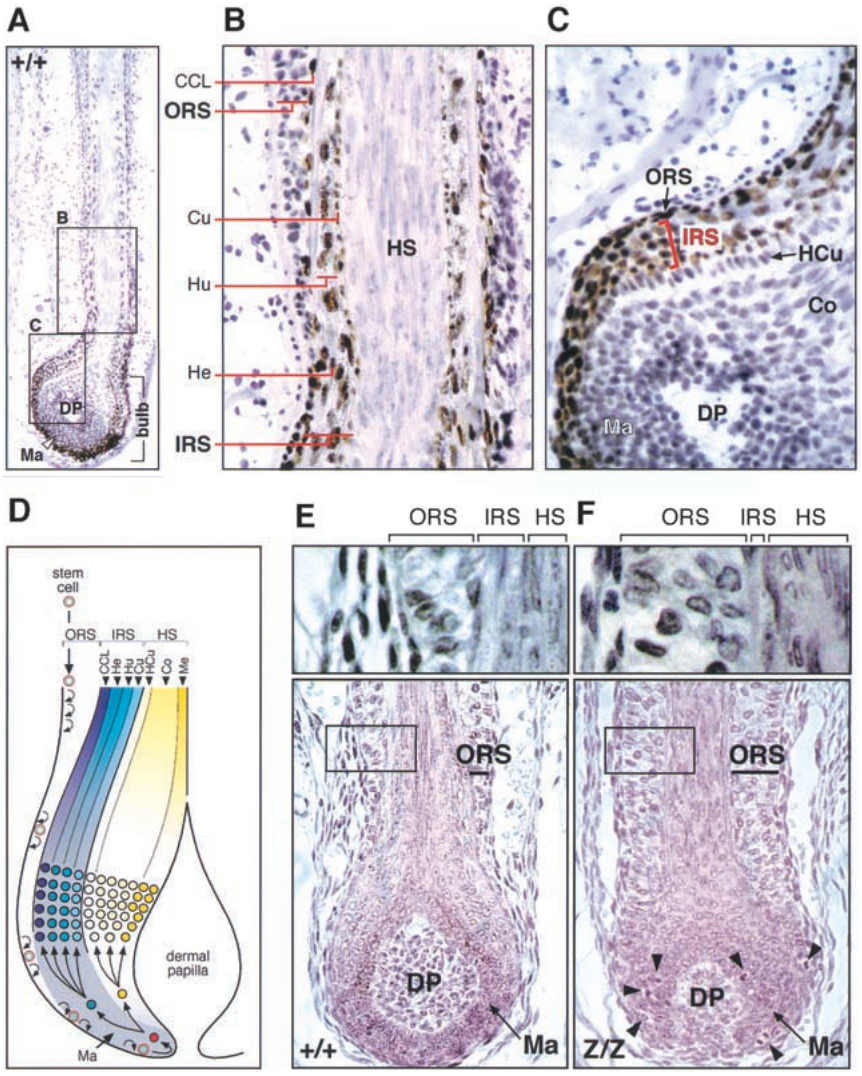

Figure 6. Abnormal differentiation of the inner root sheath in *Cutl1*$^{Z/Z}$ whisker follicles. (*A*) Expression of the CDP protein in the wild-type whisker follicle. A longitudinal section through the whisker follicle of a 5-day-old mouse was stained with the anti-CDP antibody C3HD and counterstained with hematoxylin. (*B*,*C*) Higher magnification of the areas indicated in *A*. Brown staining identifies nuclear expression of CDP in the inner root sheath (IRS) including the companion cell layer (CCL). (*D*) Schematic diagram of hair follicle differentiation. Multipotent stem cells migrate from the bulge through the outer root sheath (ORS) to the hair bulb, where they become committed to the different cell lineages of the IRS and hair shaft (HS). Gray shading denotes CDP expression in the different cell layers. (*E*,*F*) Histological sections of wild-type (*E*) and *Cutl1* mutant (*F*) whisker follicles at birth. The boxed areas are shown above at higher magnification. Mitotic cells are indicated by arrowheads. (Co) Cortex; (DP) dermal papilla; (Cu) cuticle layer of the IRS; (HCu) cuticle layer of the hair; (He) Henlé's layer; (Hu) Huxley's layer; (Ma) matrix; (Me) medulla.

cell populations on either side of Auber's line within the matrix of wild-type whisker follicles (Gambardella et al. 2000), its expression was lost in the matrix and was instead relocated to the IRS in *Cutl1* mutant follicles (Fig. 7F). In conclusion, these data show that CDP is essential for proper differentiation of the IRS by controlling the correct spatial expression of *Shh* and IRS-specific genes. Hence, CDP is a key regulator of cell-lineage specification in hair follicle development.

Discussion

Many diverse functions have been assigned to the vertebrate transcription factor CDP based on the identification of a multitude of CDP target genes, although they have not been subjected to stringent genetic tests. A previous attempt to inactivate the mouse *Cutl1* gene resulted in a hypomorphic allele, as alternative splicing skipped over the neomycin-resistance gene replacing exon 10 and thus gave rise to a CDP protein lacking Cut repeat 1 (Tufarelli et al. 1998). Homozygous *Cutl1*$^{\Delta CR1}$ mutant mice were viable and developed a coat of slightly wavy hair, although this phenotype was lost with progressing age (Tufarelli et al. 1998). Here we describe a novel *Cutl1* mutation replacing C-terminal CDP sequences with an in-frame *lacZ* gene. Mice homozygous for this mutation display a severe phenotype characterized by general growth retardation, delayed lung maturation, and impaired hair follicle development.

Expression analysis of the *lacZ* knock-in allele revealed *Cutl1* expression in the epithelial compartments of many organs that depend on epithelial–mesenchymal interactions for their development. However, we failed to detect morphological alterations of these epithelial organs in *Cutl1*$^{Z/Z}$ mice except for the lung and hair follicle. The absence of a mutant phenotype could be due to several reasons. First, *Cutl1* may indeed not be essential for the differentiation of these organs in spite of its expression. This is, however, contrasted by the fact that null mutations of the *Drosophila cut* gene result in embryonic lethality caused by multiple developmental defects (Blochlinger et al. 1988). A more likely explanation

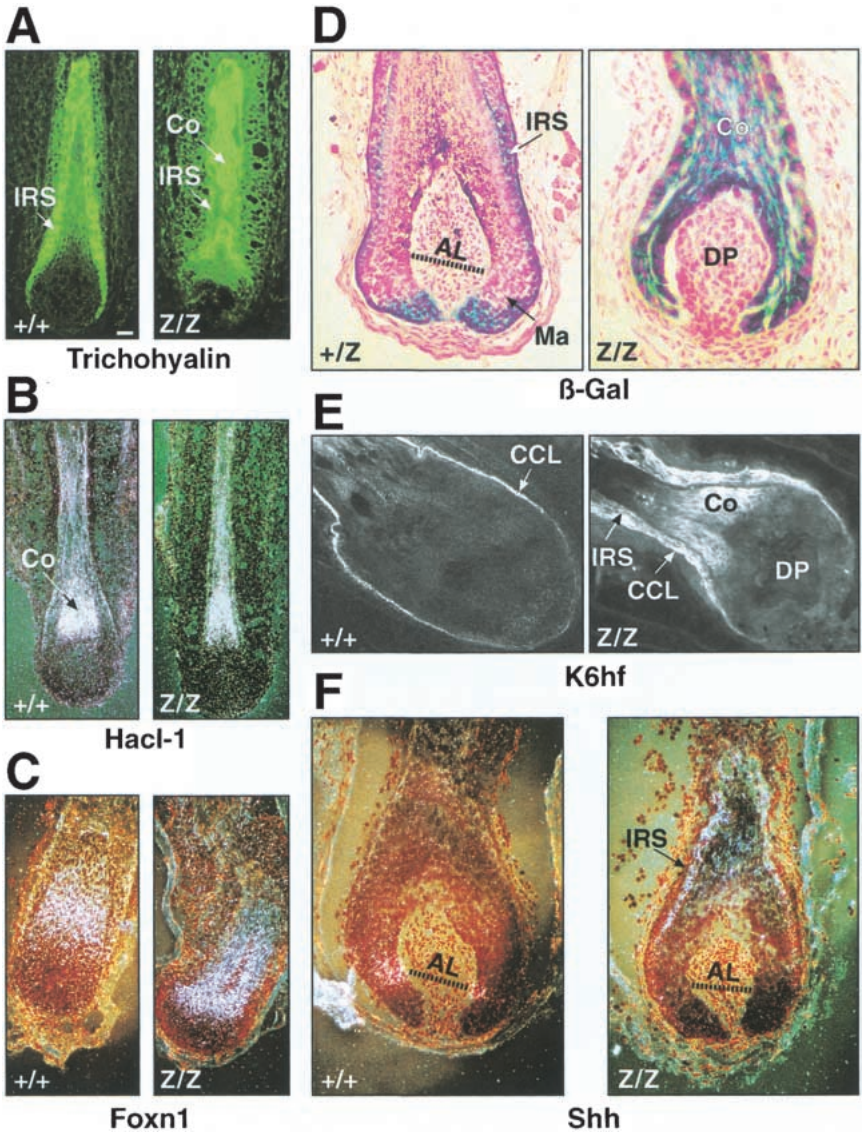

Figure 7. Deregulated expression of *Shh* and IRS-specific genes in $Cutl1^{Z/Z}$ whisker follicles. Whisker follicles in the growth phase of the hair cycle were taken from adult wild-type and *Cutl1* mutant mice and analyzed for the expression of the indicated genes by β-galactosidase staining (*D*), immunohistochemistry (*A*,*E*), and in situ hybridization (*B*,*C*,*F*). Hacl-1 (*B*) and K6hf (*E*) are cytokeratins, and trichohyalin (*A*) is a keratin-associated protein. The transcription factor Foxn1 (*H*) is also known as Whn, encoded by the *nude* gene. *Shh* (*F*) is expressed in the matrix of wild-type whisker follicles within small cell populations on either side of Auber's line (AL, dotted line), which characterizes the largest diameter of the dermal papilla (Gambardella et al. 2000). (Ma) matrix; (CCL) companion cell layer; (IRS) inner root sheath.

is provided by the existence of two vertebrate *Cutl* genes, which may fulfill redundant functions in development. Although the mouse *Cutl2* gene was reported to be exclusively expressed in the central and peripheral nervous systems (Quaggin et al. 1996), it remains a possibility that transcripts of this gene were not detected in other tissues because of the generally low expression of *Cutl* genes. In support of this, the chicken *Cutl2* gene was recently shown to be expressed in the epithelial structures of the developing kidney (Tavares et al. 2000). Analogous expression of the mouse *Cutl2* gene could therefore compensate for the loss of CDP function in kidney development of *Cutl1* mutant mice.

Finally, the $Cutl1^{Z}$ mutation could be a hypomorphic allele in view of the fact that the N-terminal 1150 amino acids of CDP are still present in the CDP–lacZ fusion protein. However, all available evidence suggests that the $Cutl1^{Z}$ mutation corresponds to a null allele, as the CDP–lacZ protein is retained in the cytoplasm and fails to function as a repressor or dominant-negative protein. Interestingly, the postmeiotic spermatids in the testis abundantly express a short CDP isoform that consists entirely of the C-terminal sequences (Vanden Heuvel et al. 1996) deleted in the $Cutl1^{Z}$ allele. In the absence of this isoform, the $Cutl1^{Z/Z}$ males were still fertile, showing that CDP is not essential for spermiogenesis. Likewise, limb development was entirely normal in $Cutl1^{Z/Z}$ mice (Fig. 2B), although misexpression experiments have recently implicated the chicken *Cutl1* gene in the control of limb morphogenesis (Tavares et al. 2000).

Essential role of Cutl1 *in growth control and lung maturation*

One prevailing hypothesis about the CDP function in hematopoiesis states that *Cutl1* expression at early stages represses lineage-specific genes, which are activated only during the CDP-negative phase of terminal

differentiation (Skalnik et al. 1991; Lievens et al. 1995; Wang et al. 1999). However, our expression analysis in hematopoietic cells failed to support this hypothesis, as expression of the *Cutl1*^{lacZ} gene was not inversely correlated with terminal differentiation in the B-lymphoid and myeloid lineages (data not shown). Moreover, the *Cutl1*^{Z} mutation neither overtly affected hematopoietic cell differentiation nor altered expression of the putative CDP target genes *CD8*α, *TCR*β, and *IgH* (data not shown).

The second prevailing hypothesis implicates CDP in the control of cell proliferation, as putative CDP target genes code for the cell-cycle-regulated Cdk inhibitor p21$^{WAF1/CIP1}$, c-Myc, thymidine kinase, and histones (for review, see Nepveu 2001). Further support was provided by the cell-cycle-dependent regulation of the DNA-binding activity and complex formation of CDP with cyclin A, Cdk2, and Rb-related proteins in cultured fibroblasts (van Wijnen et al. 1996; Coqueret et al. 1998). Contrary to expectation, primary fibroblasts established from *Cutl1*$^{Z/Z}$ embryos proliferated as well as wild-type control cells (data not shown), indicating that CDP is not a critical regulator of cell-cycle progression in fibroblasts. However, we cannot exclude that a proliferative function of CDP may be responsible for the growth-retardation phenotype of *Cutl1*$^{Z/Z}$ mice.

Lung development is initiated by the outpouching of foregut endoderm into the splanchnic mesenchyme and is subsequently guided by reciprocal epithelial–mesenchymal interactions that control the proliferation, branching, and differentiation of the lung epithelium (Burri 1999). *Cutl1* is expressed in lung epithelial cells as early as E12.5, but is dispensable for branching morphogenesis in *Cutl1*$^{Z/Z}$ embryos. However, during the saccular stage of lung development CDP is essential for differentiation of the cuboidal epithelial precursor cells into functional type I and II pneumocytes. Inbred *Cutl1*$^{Z/Z}$ mice are born with thick, nonfunctional lung epithelia and die shortly after birth from respiratory failure. A similar immature lung phenotype was observed previously in mice lacking the epidermal growth factor receptor (Sibilia and Wagner 1995), glucocorticoid receptor (Cole et al. 1995), or TGF-β3 (Kaartinen et al. 1995). However, none of these genes is under the control of CDP, as they were normally expressed in the lung epithelia of newborn *Cutl1*$^{Z/Z}$ mice (data not shown). Interestingly, the *Cutl1*^{Z} mutation on the outbred OF1 background caused a less severe delay in pneumocyte differentiation and was therefore compatible with survival beyond birth. Hence, genetic modifier loci influence the severity of the lung phenotype in different mouse strains by altering the dependency of pneumocyte differentiation on CDP function.

Cutl1-dependent cell fate specification in hair follicle development

In contrast to the lung, the *Cutl1*^{Z} mutation disrupts hair follicle development in a strain background-independent manner. The initial phase of hair follicle development, which relies on inductive interactions between selected epidermal keratinocytes and underlying dermal fibroblasts, proceeds normally in *Cutl1*$^{Z/Z}$ embryos. However, the later differentiation of stem cells into distinct lineages of the hair follicle is affected in the absence of CDP. During the growth phase of hair follicle development, the stem cells migrate from the bulge through the basal layer of the outer root sheath (ORS) to the matrix region of the bulb, where they proliferate under the influence of signals from the dermal papilla. These proliferating progenitors subsequently undergo lineage commitment, withdraw from the cell cycle, and enter one of seven vertical differentiation pathways, giving rise to the concentric layers of the IRS and hair shaft (Fig. 6D; Taylor et al. 2000; Oshima et al. 2001). The *Cutl1* expression pattern in the hair follicle is unique, as its transcription is initiated in stem cells reaching the bulb and is then maintained in the proliferating IRS progenitor cells, in the differentiating cells of the cuticle, Huxley's and Henlé's layers of the IRS, and in the adjacent companion cell layer. Although the companion cells are thought to constitute the innermost layer of the ORS, they form only few connections with other cells in the ORS (Rothnagel and Roop 1995). In contrast, however, the companion cells are in intimate contact with cells of Henlé's layer through desmosomes and gap junctions and therefore may form a slippage plane to allow the growing hair fiber to move along the ORS (Rothnagel and Roop 1995). Moreover, the elongated and vertically oriented companion cells are also morphologically and biochemically distinct from the cuboidal ORS cells, which has led to the hypothesis that the companion cells constitute an independent histological compartment of the hair follicle (Rothnagel and Roop 1995; Winter et al. 1998). The coexpression of *Cutl1* in the IRS and companion cells now strongly argues that the companion cells constitute the fourth and outermost layer of the IRS.

The IRS-specific expression of *Cutl1* is consistent with the observed reduction of IRS cell layers in the *Cutl1*$^{Z/Z}$ hair follicle, which suggests a cell-autonomous role of CDP in IRS cell differentiation. This defect in IRS formation is likely to be a primary cause for the dramatic disruption of hair follicle morphogenesis in *Cutl1*$^{Z/Z}$ mice. The IRS normally envelops the developing hair fiber and migrates upward together with it, until it cornifies upon terminal differentiation and is separated from the hair by extrusion into the infundibulum at the upper follicle end (Philpott and Paus 1998). Aberrant IRS differentiation in the *Cutl1*$^{Z/Z}$ hair follicle interferes with this normal function of the IRS and thus fails to support proper growth of the hair fiber, leading to multiple hair abnormalities.

At the molecular level, the loss of CDP function leads to the ectopic expression of IRS-specific genes (*Cutl1*, *K6hf*, *K6irs*, and *trichohyalin*) in the cortex of the hair shaft. The continued expression of the *Cutl1*^{lacZ} gene in hair shaft cells of homozygous mutants was surprising, as CDP cannot be directly involved in the repression of its own gene for the following reasons. First, CDP does

not repress its own transcription in the IRS layers of wild-type hair follicles. Second, CDP is normally not expressed in hair shaft cells and therefore is not available to repress IRS-specific genes in this compartment. It is therefore more likely that CDP is involved in regulating the expression of an non-cell-autonomous signal that instructs progenitor cells of the hair shaft lineages to inactivate the *Cutl1* gene together with the IRS-specific gene expression program. Indeed, *Shh* expression is lost in the matrix cells of *Cutl1* mutant whisker follicles, where it is normally transcribed in a ring-like fashion along Auber's line (Gambardella et al. 2000). However, the expression domain of *Shh* does not overlap with that of *Cutl1* in the matrix region (Fig. 7D,F), suggesting that CDP is indirectly involved in the activation of *Shh* in matrix cells of wild-type mice. In contrast, CDP may directly repress *Shh* transcription in IRS cells, whereas *Shh* becomes derepressed in $Cutl1^{Z/Z}$ whisker follicles. To what degree ectopic expression of *Shh* contributes to the *Cutl1* mutant phenotype is unclear at present based on published loss- and gain-of-function data. Disruption of the *Shh* gene or treatment with neutralizing anti-hedgehog antibodies revealed an essential role of Shh in controlling the down-growth and morphogenesis of the hair follicle (St-Jacques et al. 1998; Chiang et al. 1999; Wang et al. 2000). On the other hand, transient ectopic expression of *Shh* in the skin induced resting hair follicles to enter the growth phase of the next hair cycle (Sato et al. 1999). Moreover, deregulated *Shh* expression in the matrix region was previously associated with misangling of hair follicles (Gat et al. 1998), which is also observed in the *Cutl1* mutant skin. Ectopic Shh signaling emanating from IRS cells of the $Cutl1^{Z/Z}$ hair follicle could also be responsible for the observed thickening of the ORS, where *Cutl1* is not expressed. In summary, our data show that CDP uses cell-intrinsic and non-cell-autonomous mechanisms to control cell lineage specification during hair follicle morphogenesis. This function of CDP resembles the role of *Drosophila* Cut in specifying cell fates during peripheral nervous system development (Blochlinger et al. 1988, 1991).

Materials and methods

Generation of Cutl1 *mutant mice*

The *Cutl1* targeting vector was assembled in plasmid pGNA containing a polylinker with appropriate restriction sites. A 1.8-kb *Bsa*I fragment (short homology arm) of the *Cutl1* gene was linked in the Cut repeat 3 exon 22 to the *lacZ* gene of pGNA via an adaptor oligonucleotide resulting in the following amino acid insertion (underlined): LFGETLEKIFRNSAKKKRKVEDPKDFPSELLSFLSPSLALAVVL. A 3.8-kb *Sph*I–*Bam*HI fragment (long homology arm) encompassing *Cutl1* intron 23 was then inserted together with a 1.9-kb *Xba*I–*Not*I fragment containing the *tk* gene. *Not*I-linearized DNA (15 µg) of the pGNA–Cutl1 targeting vector was electroporated into E14.1 ES cells (1×10^7) followed by selection with 150 µg/mL of bioactive G418. Individual clones were screened by PCR for homologous recombination, and PCR-positive clones were verified by Southern blot analysis (Fig. 1A). Two of four correctly targeted ES cell clones gave rise to germ-line transmission after injection into C57BL/6 blastocysts. The $Cutl1^Z$ allele was maintained on the C57BL/6 × 129/Sv background as well as back-crossed into the C3H/He and albino OF1 strains (Iffa Credo, France). *Cutl1* mutant mice were genotyped by PCR with the following primers: (1) 5′-TGCTCATCCACCTGCCTCAATGTC-3′, (2) 5′-ATCCATCAGCTTCTCCACATTGTT-3′, and (3) 5′-TCCTGTAGCCAGCTTTCATCAACA-3′. The wild-type and $Cutl1^Z$ alleles gave rise to PCR products of 615 bp (primers 1/2) and 962 bp (primers 1/3), respectively.

Histological analysis and β*-galactosidase staining*

Embryos or dissected organs were fixed in 4% formaldehyde/PBS, and 7-µm paraffin-embedded sections were stained with eosin and hematoxylin. For β-galactosidase staining, the samples were fixed for 30 min at room temperature in buffer X (0.2% gluteraldehyde, 0.1 M NaH_2PO_4 at pH 7.2, 5 mM EGTA, 2 mM $MgCl_2$), washed in buffer W (0.1 M NaH_2PO_4 at pH 7.2, 2 mM $MgCl_2$, 0.01% deoxycholate, 0.03% NP40), and sequentially incubated in solutions of 10%–30% sucrose. The samples were embedded in Tissue-Tek O.C.T. medium (Sakura) and quick-frozen in liquid nitrogen. Cyrosections were postfixed for 10 min in buffer X, stained with 0.67 mg/mL X-gal (5-bromo-4-chloro-3-indolyl-β-D-galactoside) in buffer W, and counterstained with 0.1% Nuclear Fast Red in 5% aluminum sulfate.

Anti-CDP antibody

A 432-bp PCR fragment was amplified from pRK5–mCDP with primers 5′-gcgggatccCAGGGTTCTGTCTCCGACCTC-3′ and 5′-gcgggatcctta GCGGCGAATCCGAGACCTGTAATT-3′ and inserted into the *Bam*HI site of the bacterial expression vector pETH-2a (Adams et al. 1992). The recombinant CDP polypeptide (starting with QGSV in Cut repeat 3 and ending with PIRR in the homeodomain) was expressed, purified, and injected into rabbits to generate the polyclonal anti-CDP serum C3HD, as described (Adams et al. 1992).

Immunohistochemistry

Cryosections of whisker follicles were stained with the anti-trichohyalin antibody AE15 (Wang et al. 2000) and anti-K6hf antibody Bax-1 (Winter et al. 1998), as described. For CDP staining, cryosections were incubated overnight at 4°C with the affinity-purified C3HD antibody (0.3 µg/mL), which was detected with biotinylated goat anti-rabbit IgG followed by DAB staining with the Vectastain ABC kit (Vector Labs).

Primary fibroblasts, established from $Cutl1^{+/Z}$ embryos at E13.5 by the 3T3 protocol, were fixed in 1% formaldehyde/PBS at 25°C for 20 min, blocked in 3% BSA/PBS for 30 min, and incubated overnight at 4°C with the affinity-purified C3HD antibody (0.3 µg/mL) and a biotinylated anti-β-Gal antibody (Sigma). Polyclonal and biotinylated antibodies were detected by incubation with a Cy5-labeled goat anti-rabbit antibody (Jackson Laboratories) and Alexa488-conjugated avidin (Molecular Probes), respectively.

EM and histological analyses of the lung

The trachea of anesthetized mice were cannulated, and the lungs were fixed by intratracheal instillation of a 2.5% KH_2PO_4-buffered glutaraldehyde solution (pH 7.4, 360 mOsm) after provoking a pneumothorax by puncturing the diaphragm. After dissection, the lungs were fixed in the same solution for a further

24 h at 4°C. Paraffin-embedded 4-µm sections of the left lobe were stained with fuchsin for light microscopic investigation. For EM analysis, the right lobe was postfixed in 1% osmium tetroxide, contrasted in 0.5% uranyl acetate, and embedded in Epon 812. Ultrathin sections (80 nm) on 22-mesh grids were stained with uranyl acetate and lead citrate, followed by examination in a Philips EM 300.

In situ hybridization

Whisker follicles of albino OF1 mice were analyzed by in situ hybridization with gene-specific ^{33}P-labeled antisense oligonucleotides (45 nt) as described (Wang et al. 2000). The oligonucleotide sequences are available on request (busslinger@nt.imp.univie.ac.at).

Hormone measurements

Growth hormone (GH) and thyroid-stimulating hormone (TSH) were measured in the sera of 2-week-old OF1 mice by radioimmunoassay at the Institute of National Hormone and Pituitary Program (Torrance, CA).

Cell transfection assay

The full-length *CDP* cDNA insert of pRK5–mCDP was isolated as a 4.9-kb *Xba*I–*Cla*I fragment by RT–PCR from mouse 70Z/3 pre-B cells. pRK5–mCDP–lacZ was generated by inserting a 3087-bp *Xba*I–*Dra*III fragment (N-terminal CDP sequences) of pRK5–mCDP, a 378-bp *Dra*III–*Xho*I PCR fragment (CDP–lacZ linker), and a 3552-bp *Xho*I–*Bam*HI fragment (C-terminal lacZ sequences) of pGNA–Cutl1 into the expression vector pRK5. The *Dra*III–*Xho*I linker fragment was obtained by RT–PCR from lung RNA of *Cutl1*$^{Z/Z}$ embryos. The promoter of SP1-γ–TATA–GH (Lievens et al. 1995) was PCR-amplified and inserted into pGL3–Basic to generate SP1-γ–TATA–luc. These DNAs were transiently transfected into NIH 3T3 cells by the Lipofect-AMINE PLUS Reagent (GIBCO BRL).

Accession number

The mouse CDP cDNA sequence of pRK5–mCDP was submitted to DBBJ/EMBL/GenBank with accession no. AY037807.

Acknowledgments

We thank E. Neufeld for the SP1-γ–TATA–GH construct, A.F. Parlow for hormone measurements, A. Nepveu for the N(-861) antibody, L. Langbein for the K6hf and K6irs antibodies, C. Theußl for blastocyst injection, and G. Schaffner for DNA sequencing. This research was supported by Boehringer Ingelheim, the Austrian Industrial Research Promotion Fund, ARC and INSERM (grant CRI 9602 to Y.B.), and the French Ministry of Education, Research and Technology (student fellowship for L.G.).

The publication costs of this article were defrayed in part by payment of page charges. This article must therefore be hereby marked "advertisement" in accordance with 18 USC section 1734 solely to indicate this fact.

References

Adams, B., Dörfler, P., Aguzzi, A., Kozmik, Z., Urbánek, P., Maurer-Fogy, I., and Busslinger, M. 1992. *Pax-5* encodes the transcription factor BSAP and is expressed in B lymphocytes, the developing CNS, and adult testis. *Genes & Dev.* **6:** 1589–1607.

Banan, M., Rojas, I.C., Lee, W.-H., King, H.L., Harriss, J.V., Kobayashi, R., Webb C.F., and Gottlieb, P.D. 1997. Interaction of the nuclear matrix-associated region (MAR)-binding proteins, SATB1 and CDP/Cux, with a MAR element (L2a) in an upstream regulatory region of the mouse *CD8a* gene. *J. Biol. Chem.* **272:** 18440–18452.

Barberis, A., Superti-Furga, G., and Busslinger, M. 1987. Mutually exclusive interaction of the CCAAT-binding factor and of a displacement protein with overlapping sequences of a histone gene promoter. *Cell* **50:** 347–359.

Blochlinger, K., Bodmer, R., Jack, J., Jan, L.Y., and Jan, Y.N. 1988. Primary structure and expression of a product from *cut*, a locus involved in specifying sensory organ identity in *Drosophila*. *Nature* **333:** 629–635.

Blochlinger, K., Jan, L.Y., and Jan, Y.N. 1991. Transformation of sensory organ identity by ectopic expression of Cut in *Drosophila*. *Genes & Dev.* **5:** 1124–1135.

Burri, P.H. 1999. Lung development and pulmonary angiogenesis. In *Lung development* (eds. C. Gaultier et al.), pp. 122–151. Oxford University Press, New York, NY.

Chattopadhyay, S., Whitehurst, C.E., and Chen, J. 1998. A nuclear matrix attachment region upstream of the T cell receptor β gene enhancer binds Cux/CDP and SATB1 and modulates enhancer-dependent reporter gene expression but not endogenous gene expression. *J. Biol. Chem.* **273:** 29838–29846.

Chiang, C., Swan, R.Z., Grachtchouk, M., Bolinger, M., Litingtung, Y., Roberston, E.K., Cooper, M.K., Gaffield, W., Westphal, H., Beachy, P.A., et al. 1999. Essential role of *Sonic hedgehog* during hair follicle morphogenesis. *Dev. Biol.* **205:** 1–9.

Cole, T.J., Blendy, J.A., Monaghan, A.P., Krieglstein, K., Schmid, W., Aguzzi, A., Fantuzzi, G., Hummler, E., Unsicker, K., and Schütz, G. 1995. Targeted disruption of the glucocorticoid receptor gene blocks adrenergic chromaffin cell development and severely retards lung maturation. *Genes & Dev.* **9:** 1608–1621.

Coqueret, O., Bérubé, G., and Nepveu, A. 1998. The mammalian Cut homeodomain protein functions as a cell-cycle-dependent transcriptional repressor which downmodulates p21WAF1/CIP1/SDI1 in S phase. *EMBO J.* **17:** 4680–4694.

Gambardella, L., Schneider-Maunoury, S., Voiculescu, O., Charnay, P., and Barrandon, Y. 2000. Pattern of expression of the transcription factor Krox-20 in mouse hair follicle. *Mech. Dev.* **96:** 215–218.

Gat, U., DasGupta, R., Degenstein, L., and Fuchs, E. 1998. De novo hair follicle morphogenesis and hair tumors in mice expressing a truncated β-catenin in skin. *Cell* **95:** 605–614.

Jackson, S.M. and Blochlinger, K. 1997. *cut* interacts with *Notch* and Protein kinase A to regulate egg chamber formation and to maintain germline cyst integrity during *Drosophila* oogenesis. *Development* **124:** 3663–3672.

Kaartinen, V., Voncken, J.W., Shuler, C., Warburton, D., Bu, D., Heisterkamp, N., and Groffen, J. 1995. Abnormal lung development and cleft palate in mice lacking TGF-β3 indicates defects of epithelial–mesenchymal interaction. *Nat. Genet.* **11:** 415–421.

Li, S., Moy, L., Pittman, N., Shue, G., Aufiero, B., Neufeld, E.J., LeLeiko, N.S., and Walsh, M.J. 1999. Transcriptional repression of the cystic fibrosis transmembrane conductance regulator gene, mediated by CCAAT displacement protein/*cut* homolog, is associated with histone deacetylation. *J. Biol. Chem.* **274:** 7803–7815.

Lievens, P.M.J., Donady, J.J., Tufarelli, C., and Neufeld, E.J.

1995. Repressor activity of CCAAT displacement protein in HL-60 myeloid leukemia cells. *J. Biol. Chem.* **270:** 12745–12750.

Lievens, P.M.J., Tufarelli, C., Donady, J.J., Stagg, A., and Neufeld, E.J. 1997. CASP, a novel, highly conserved alternative-splicing product of the CDP/*cut*/*cux* gene, lacks cut-repeat and homeo DNA-binding domains, and interacts with full-length CDP in vitro. *Gene* **197:** 73–81.

Ludlow, C., Choy, R., and Blochlinger, K. 1996. Functional analysis of *Drosophila* and mammalian cut proteins in files. *Dev. Biol.* **178:** 149–159.

Mailly, F., Bérubé, G., Harada, R., Mao, P.-L., Phillips, S., and Nepveu, A. 1996. The human Cut homeodomain protein can repress gene expression by two distinct mechanisms: Active repression and competition for binding site occupancy. *Mol. Cell. Biol.* **16:** 5346–5357.

Micchelli, C.A., Rulifson, E.J., and Blair, S.S. 1997. The function and regulation of *cut* expression on the wing margin of *Drosophila*: Notch, Wingless and a dominant negative role for Delta and Serrate. *Development* **124:** 1485–1495.

Moon, N.S., Berube, G., and Nepveu, A. 2000. CCAAT displacement activity involves Cut repeats 1 and 2 and not the Cut homeodomain. *J. Biol. Chem.* **275:** 31325–31334.

Nepveu, A. 2001. Role of the multifunctional CDP/Cut/Cux homeodomain transcription factor in regulating differentiation, cell growth and development. *Gene* **270:** 1–15.

Neufeld, E.J., Skalnik, D.G., Lievens, P.M.-J., and Orkin, S.H. 1992. Human CCAAT displacement protein is homologous to the *Drosophila* homeoprotein, cut. *Nat. Genet.* **1:** 50–55.

Oshima, H., Rochat, A., Kedzia, C., Kobayashi, K., and Barrandon, Y. 2001. Morphogenesis and renewal of hair follicles from adult multipotent stem cells. *Cell* **104:** 233–245.

Philpott, M. and Paus, R. 1998. Principles of hair follicle morphogenesis. In *Molecular basis of epithelial appendage morphogenesis* (ed. C.-M. Chuong), pp. 75–110. R.G. Landes, Austin, TX.

Quaggin, S.E., Vanden Heuvel, G.B., Golden, K., Bodmer, R., and Igarashi, P. 1996. Primary structure, neural-specific expression, and chromosomal localization of *Cux-2*, a second murine homeobox gene related to *Drosophila cut*. *J. Biol. Chem.* **271:** 22624–22634.

Rothnagel, J.A. and Roop, D.R. 1995. Hair follicle companion layer: Reacquainting an old friend. *J. Invest. Dermatol.* **104:** 42S–43S.

Sato, N., Leopold, P.L., and Crystal, R.G. 1999. Induction of the hair growth phase in postnatal mice by localized transient expression of Sonic hedgehog. *J. Invest. Dermatol.* **104:** 855–864.

Sibilia, M. and Wagner, E.F. 1995. Strain-dependent epithelial defects in mice lacking the EGF receptor. *Science* **269:** 234–238.

Skalnik, D.G., Strauss, E.C., and Orkin, S.H. 1991. CCAAT displacement protein as a repressor of the myelomonocytic-specific gp91–phox gene promoter. *J. Biol. Chem.* **266:** 16736–16744.

St-Jacques, B., Dassule, H.R., Karavanova, I., Botchkarev, V.A., Li, J., Danielian, P.S., McMahon, J.A., Lewis, P.M., Paus, R., and McMahon, A.P. 1998. Sonic hedgehog signaling is essential for hair development. *Curr. Biol.* **8:** 1058–1068.

Superti-Furga, G., Barberis, A., Schaffner, G., and Busslinger, M. 1988. The –117 mutation in Greek HPFH affects the binding of three nuclear factors to the CCAAT region of the γ-*globin* gene. *EMBO J.* **7:** 3099–3107.

Tavares, A.T., Tsukui, T., and Izpisúa Belmonte, J.C. 2000. Evidence that members of the Cut/Cux/CDP family may be involved in AER positioning and polarizing activity during chick limb development. *Development* **127:** 5133–5144.

Taylor, G., Lehrer, M.S., Jensen, P.J., Sun, T.-T., and Lavker, R.M. 2000. Involvement of follicular stem cells in forming not only the follicle but also the epidermis. *Cell* **102:** 451–461.

Tufarelli, C., Fujiwara, Y., Zappulla, D.C., and Neufeld, E.J. 1998. Hair defects and pup loss in mice with targeted deletion of the first cut repeat domain of the *Cux/CDP* homeoprotein gene. *Dev. Biol.* **200:** 69–81.

Vanden Heuvel, G.B., Quaggin, S.E., and Igarashi, P. 1996. A unique variant of a homeobox gene related to *Drosophila cut* is expressed in mouse testis. *Biol. Reprod.* **55:** 731–739.

van Wijnen, A.J., van Gurp, M.F., de Ridder, M.C., Tufarelli, C., Last, T.J., Birnbaum, M., Vaughan, P.S., Giordano, A., Krek, W., Neufeld, E.J., et al. 1996. CDP/*cut* is the DNA-binding subunit of histone gene transcription factor HiNF-D: A mechanism for gene regulation at the G_1/S phase cell cycle transition point independent of transcription factor E2F. *Proc. Natl. Acad. Sci.* **93:** 11516–11521.

Wang, Z., Goldstein, A., Zong, R.T., Lin, D., Neufeld, E.J., Scheuermann, R.H., and Tucker, P.W. 1999. Cux/CDP homeoprotein is a component of NF-μNR and represses the immunoglobulin heavy chain intronic enhancer by antagonizing the bright transcription activator. *Mol. Cell. Biol.* **19:** 284–295.

Wang, L.C., Liu, Z.-Y., Gambardella, L., Delacour, A., Shapiro, R., Yang, J., Sizing, I., Rayhorn, P., Garber, E.A., Benjamin, C.D., et al. 2000. Conditional disruption of hedgehog signaling pathway defines its critical role in hair development and regeneration. *J. Invest. Dermatol.* **114:** 901–908.

Whiting, D.A. 1994. Hair shaft defects. In *Disorders of hair growth: Diagnosis and treatment* (ed. E.A. Olsen), pp. 91–137. McGraw-Hill, New York, NY.

Winter, H., Langbein, L., Praetzel, S., Jacobs, M., Rogers, M.A., Leight, I.M., Tidman, N., and Schweizer, J. 1998. A novel human type II cytokeratin, K6hf, specifically expressed in the companion layer of the hair follicle. *J. Invest. Dermatol.* **111:** 955–962.

Zeng, W.R., Soucie, E., Moon, N.S., Martin-Soudant, N., Bérubé, G., Leduy, L., and Nepveu, A. 2000. Exon/intron structure and alternative transcripts of the *CUTL1* gene. *Gene* **241:** 75–85.